

PACS numbers: 42.55.Px; 41.75.Fr; 85.35.Be; 42.60.Lh
DOI: 10.1070/QE2015v045n07ABEH015780

Pulsed electron-beam-pumped laser based on AlGaN/InGaN/GaN quantum-well heterostructure

N.A. Gamov, E.V. Zhdanova, M.M. Zverev, D.V. Peregoudov, V.B. Studenov, A.V. Mazalov, V.A. Kureshov, D.R. Sabitov, A.A. Padalitsa, A.A. Marmalyuk

Abstract. **The parameters of pulsed blue-violet ($\lambda \approx 430$ nm at $T = 300$ K) lasers based on an AlGaN/InGaN/GaN structure with five InGaN quantum wells and transverse electron-beam pumping are studied. At room temperature of the active element, the minimum electron energy was 9 keV and the minimum threshold electron beam current density was 8 A cm^{-2} at an electron energy of 18 keV.**

Keywords: *electron-beam-pumped laser, quantum-well structure, quantum well.*

Electron-beam pumping of semiconductor lasers [1] allows them to operate in specific regimes taking place only in the lasers of this type. In particular, there exists the possibility of successive or simultaneous emission of pulses at different wavelengths, angular laser scanning, and synchronisation of light and triggering pulses with nanosecond accuracy [1, 2]. The use of quantum-well semiconductor structures as active elements of pulsed electron-beam-pumped lasers allowed one to considerably improve laser characteristics. For example, the energy and the threshold current density of the pump electron beam in lasers based on quantum-well structures are much lower than in lasers based on single crystals. This facilitated the development of miniature IR and visible light sources [3–5]. The electron energy U needed for room-temperature operation of green lasers based on ZnSe-containing structures, as well as of IR lasers based on GaAs/InGaAs/AlGaAs structures, was decreased to 3.5–10 keV [6, 7]. Laser arrays consisting of optically isolated lasers pumped by a common electron beam can emit green light with a peak power exceeding 600 W [8]. These lasers can be used in optical location systems, communications, medicine, biology, etc. The electron-beam-pumped lasers operate without a p–n junction, which makes it possible to use the structures based on materials in which the p-type conductivity is difficult to create. First of all, these are the structures emitting in the UV region, in particular, the structures based on indium, gallium, and aluminium nitrides.

In recent times, the compounds based on AlGaN have been extensively studied and are now widely used for the development of illuminating lamps and various electronic and optoelectronic devices. At the same time, electron-beam-pumped laser based on these compounds are studied rather poorly. For the first time, the operation of an electron-beam-pumped laser based on an InGaN/GaN structure was reported in [9]. The authors of [9] studied an InGaN/GaN structure with 30 InGaN quantum wells (QWs) and, in the case of cooling this structure by liquid nitrogen, achieved the threshold density $J_{th} = 60$ A cm^{-2} at the electron energy $U =$ 50 keV. At room temperature of the sample, the threshold density was $J_{th} = 200–300$ A cm^{-2} at $U = 150$ keV. Recently [10, 11], we achieved lasing ($T = 300$ K) in an InGaN/GaN structure with the minimum J_{th} of 40 A cm^{-2} at $U = 19$ keV. The waveguide was formed by $In_{0.02}Ga_{0.98}N$ layers (the outer layer was 200 nm thick), and the active region consisted of five $In_{0.17}Ga_{0.83}N$ QWs separated by GaN barriers.

In this publication, we present the results of investigations of a blue-violet laser based on an AlGaN/InGaN/GaN structure with an improved design, namely, with a decreased thickness of the outer surface layer bounding the waveguide.

The penetration depth of electrons into a sample depends on their energy U, and, at $U < 15$ keV, the maximum of the pump energy loss distribution in the sample is distant from the structure surface by less than 200 nm [12]. It is this thickness of the outer boundary layer that was previously used in [10, 11]. In the present work, in order to decrease the pump electron energy, we have grown a structure with a thinner outer boundary layer. The structures for lasers were grown by MOC hydride epitaxy on a sapphire substrate. The waveguide of the structure was formed by layers of $Al_{0.2}Ga_{0.8}N$ (outer layer with a thickness of 20 nm) and $Al_{0.1}Ga_{0.9}N$ (inner layer 580 nm thick). The active region consisted of five $In_{0.11}Ga_{0.89}N$ QWs (2.5 nm) separated by GaN barriers (10 nm). The total thickness of the waveguide layer was about 430 nm. The scheme of the structure is shown in Fig. 1. We used transverse pumping; the laser cavities with a length of 0.5–1.2 mm were formed by cleaving. For pumping, we used a pulsed electron beam with electron energy up to 18 keV at a pulse duration of about 300 ns. The pulse repetition rate was 1.5 Hz. The sample was mounted on a copper holder in a vacuum chamber evacuated by a turbomolecular pump. In some cases, the structure was cooled using an MCMP-150H-5/2 microcryogenic system. An electron beam was focused by a magnetic lens on a slit, which confined the pump region of the active element and was placed in the immediate vicinity of the sample. The pulses of the laser under study were recorded using a

N.A. Gamov, E.V. Zhdanova, M.M. Zverev, D.V. Peregoudov, V.B. Studenov Moscow State Institute of Radio-Engineering, Electronics and Automation (Technical University), prosp. Vernadskogo 78, 119454 Moscow, Russia; e-mail: mzverev@mail.ru;
A.V. Mazalov, V.A. Kureshov, D.R. Sabitov, A.A. Padalitsa OJSC 'M.F. Stel'makh Polyus Research Institute', ul. Vvedenskogo 3, Bld.1, 117342 Moscow, Russia;
A.A. Marmalyuk OJSC 'M.F. Stel'makh Polyus Research Institute', ul. Vvedenskogo 3, Bld. 1, 117342 Moscow, Russia; National Nuclear University 'MEPhI', Kashirskoe sh. 31, 115549 Moscow, Russia

Received 9 February 2015; revision received 27 March 2015
Kvantovaya Elektronika **45** (7) 601–603 (2015)
Translated by M.N. Basieva

calibrated coaxial FEK-22 photocell and a Tektronix TDS 3032B oscilloscope, which also measured the pump electron current pulse. The laser spectra were recorded using an S100 spectrometer with a concave diffraction grating. The lasing threshold was determined visually by the appearance of a bright light point on the face of the laser sample.

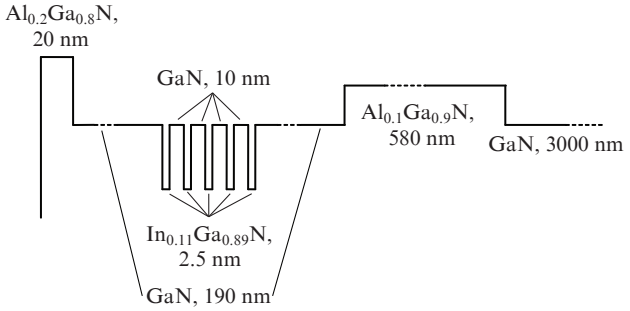

Figure 1. Scheme of the laser structure.

At room temperature of the sample, the minimum electron energy U at which we managed to obtain lasing was equal to 9 keV. With increasing U from 9 to 18 keV, the threshold current density J_{th} monotonically decreased from 11 to 8 A cm^{-2} at the laser cavity length $L = 0.6$ mm (Fig. 2). With decreasing temperature, the threshold current density for a laser with $L = 0.6$ mm decreased to $J_{th} \approx 5.5$ A cm^{-2} at $T = 180$ K and 4 A cm^{-2} at $T < 50$ K (Fig. 3). Within the range $T = 300-200$ K, the threshold current density linearly decreases with temperature. Figure 4 presents the dependence of the laser peak power (from one surface) on the pump electron current density. The maximum peak power for $L = 0.6$ mm and $U = 17$ keV was about 3 W.

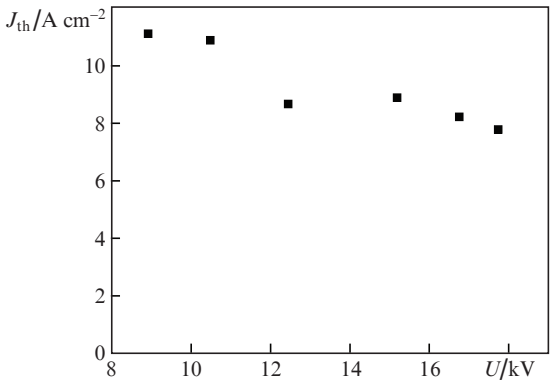

Figure 2. Dependence of the threshold current density on the pump electron energy ($T = 300$ K, $L = 0.6$ mm).

The laser wavelength varied by 1–2 nm depending on the cavity length and the pump electron energy and current density and was 429 nm at $L = 1$ mm and $T = 300$ K; the laser line half-width was 1.5–2 nm (Fig. 5). Lasing was observed at a wavelength near the luminescence peak. The laser radiation was polarised in the plane of the structure with a polarisation degree no lower than 0.95.

We calculated the spatial distribution of the carrier concentration in the structure, the carrier accumulation efficiency

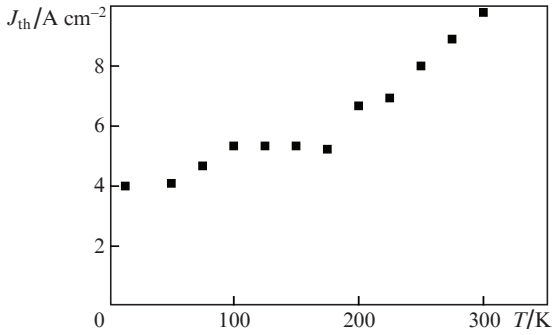

Figure 3. Dependence of the threshold current density on the sample temperature (electron energy $U = 15$ keV, $L = 0.6$ mm).

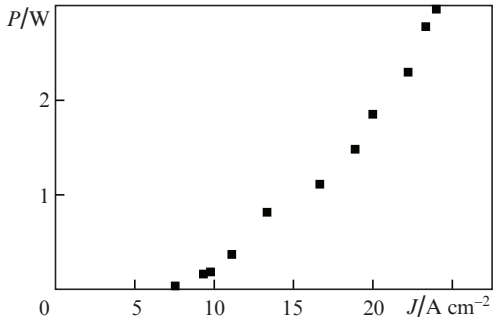

Figure 4. Dependence of the pulse power on the electron beam current density ($U = 17$ keV, $L = 0.6$ mm).

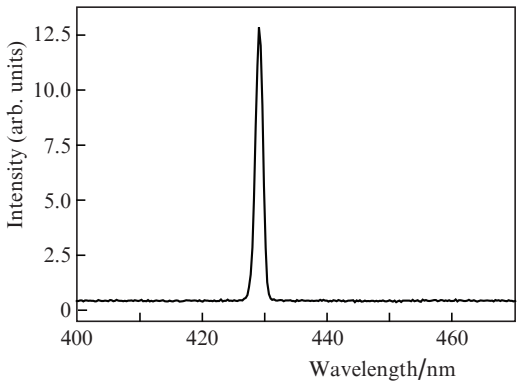

Figure 5. Laser emission spectrum ($U = 16$ keV, $L = 1$ mm).

in different QWs, and the dependence of the threshold current density on the pump electron energy and on the position of the active layer in the waveguide. The calculations were performed taking into account the diffusion of carriers and their drift in the internal fields of the structure, as well as the field distribution of the transverse electromagnetic mode in the waveguide [13]. The parameters of layers (diffusion length, lifetime, mobility of holes, refractive index) were chosen according to the data given in [14, 15]. The surface recombination coefficients s were taken to be 10 m s^{-1} at all internal interfaces and 10000 m s^{-1} at the free boundary.

Figure 6 shows the dependences of the carrier accumulation efficiency in QWs on the electron energy. The carrier accumulation efficiency was determined as the ratio of the concentration of carriers in a particular well to the total con-

centration in all the layers of the structure. Figure 6 demonstrates redistribution of accumulation efficiency in different QWs with increasing electron energy and, hence, increasing depth of electron penetration into the structure. At low electron energies, the accumulation efficiency for the first (closest to the surface) well is maximum and decreases as the beam energy increases to above 6 keV. At $U = 12$ keV, the accumulation efficiencies for the first and the last (fifth) wells become identical and then, with a further increase in U, the concentration of carriers in the last well becomes higher than in the others.

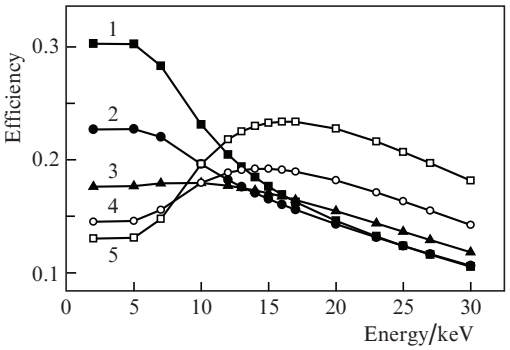

Figure 6. Calculated dependences of the nonequilibrium carrier accumulation efficiency in different QWs on the pump electron energy. The figures denote the QW numbers; well No. 1 is closest to the structure surface.

Figure 7 presents the dependence of the threshold current density on the pump electron energy calculated for structures with one and five QWs. It is seen that J_{th} monotonically decreases with increasing energy within 9–18 keV, which agrees with experiment (Fig. 2). At the same time, the threshold current density for the structure with one QW is considerably (several times) lower than for the structure with five wells. Thus, to further decrease the threshold current density, it is preferable to use structures with a single QW.

Note that the minimum pump electron energies and threshold current densities achieved in this work for lasers based on the AlGaN/InGaN/GaN structure considerably exceed the values obtained for lasers based on ZnSe-containing structures [6], as well as on the structures based on GaAs/ InGaAs [7]. The parameters of electron-pumped blue-violet lasers based on indium, gallium and aluminium nitrides can be further improved both by decreasing the number of structural defects and by optimising the laser structure design.

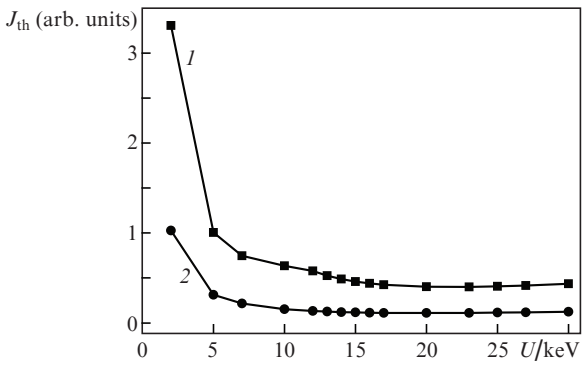

Figure 7. Dependences of the threshold current density on the pump electron energy calculated for the structures with (*1*) five and (*2*) one QW.

Thus, we demonstrated the possibility of creating pulsed blue-violet lasers based on indium, gallium and aluminium nitrides, which operate at room temperature of the active element under pumping by an electron beam with a relatively low energy (9–18 keV).

Acknowledgements. This work was supported by the Russian Foundation for Basic Research (Grant No. 13-02-00604) and by the Ministry of Science and Education (Project No. 3.611. 2014/K).

References

1. Bogdankevich O.V., Darznek S.A., Eliseev P.G. *Poluprovodnikovye lasery* (Semiconductor Lasers) (Moscow: Nauka, 1976).
2. Zverev M., Ivanov S., Olikhov I. *Elekrtronika: Nauka, Tekhnologiya, Biznes*, (4), 66 (2006).
3. Molva E., Accomo R., Labrunie G., Cibert J., Bodin C., Dang L.S., Fenillet G. *Appl. Phys. Lett*., **62**, 796 (1993).
4. Herve D., Molva E., Vanzetti L., Sorba L., Franciosi A. *Electron. Lett*., **31** (6), 459 (1995).
5. Herve D., Accomo R., Molva E., Vanzetti L., Paggel J.J., Sorba L., Francioci A. *Appl. Phys. Lett*., **67** (15), 2144 (1995).
6. Zverev M.M., Gamov N.A., Zhdanova E.V., Peregudov D.V., Studenov V.B., Ivanov S.V., Gronin S.I., Sedova I.V., Sorokin S.V., Kop'ev P.S. *Pis'ma Zh. Tekh. Fiz*., **33** (24), 1 (2007).
7. Zverev M.M., Gamov N.A., Zhdanova E.V., Ladugin M.A., Marmalyuk A.A., Peregudov D.V., Studenov V.B. *Opt. Spectrosk*., **111** (2), 212 (2011).
8. Zverev M.M., Ivanov S.V., Gamov N.A., Zdanova E.V., Studionov V.B., Peregoudov D.V., Sedova I.V., Gronin S.V., Sorokin S.V., Kop'ev P.S., Olikhov I.M. *Phys. Stat. Sol. B*, **247** (6), 1561 (2010).
9. Kozlovsky V.I., Krysa A.B., Skyasyrsky Y.K., Popov Y.M., Abare A., Mack M.P., Keller S., Mishra U. K., Coldren L., Steven DenBaars, Tiberi Michael D., George T. *MRS Internet J. Nitride Semicond. Res*., **2**, 38 (1997).
10. Gamov N.A., Zhdanova E.V., Zverev M.M., Peregudov D.V., Studenov V.B., Mazalov A.V., Kureshov V.A., Sabitov D.R., Padalitsa A.A., Marmalyuk A.A. *Trudy Intern. konf. 'Fundamental'nye problemy radioelektronnogo priborostroeniya'* (Proc. Int. Conf 'Fundamental Problems of Radioelectronics') (INTERMATIC-2012) (Moscow, 2012) p. 19.
11. Zverev M.M., Gamov N.A., Zhdanova E.V., Peregudov D.V., Studenov V.B., Mazalov A.V., Kureshov V.A., Sabitov D.R., Padalitsa A.A., Marmalyuk A.A. *Tezisy Dokl. 9 Vseros. Konf. 'Nitridy galliya, indiya i aluminiya: structury i pribory'* (Abstracts of the 9th All-Russian Conf. 'Aluminium, Indium and Gallium Nitrides: Structure and Devices') (Moscow, 2013) p. 13.
12. Gusev A.L., Zverev M.M., Ivanov S.V., Tarasov M.D. *Al'ternativnaya Energetika i Ekologiya*, (2), 102 (2011).
13. Zverev M.M., Gamov N.A., Zdanova E.V., Studionov V.B., Peregoudov D.V., Ivanov S.V., Sorokin S.V., Sedova I.V., Gronin S.V., Kop'ev P.S. *Proc. 7th Internat. Symp. 'Nanostructures: Physics and Technology'* (Minsk, Belarus, 2009) p. 35.
14. http://www.ioffe.ru/SVA/NSM/Semicond/GaN/.
15. Webb-Wood G., Ozgur U., Everitt H.O., Yun F., Morkoc H. *Phys. Stat. Sol. (a)*, **188** (2), 793 (2001).